Generation of Cellular Micropatterns on a Single-Layered Graphene Film

Daewha Hong, KiEun Bae, Sangjin Yoo, Kyungtae Kang, Byoungwook Jang, Jinkyu Kim, Sehun Kim, Seokwoo Jeon, Yoonkey Nam, Yang-Gyun Kim, Insung S. Choi*

Micropatterns of fibroblast and hippocampal neurons are generated on a single-layered graphene substrate. A large-area (1 cm × 1 cm) graphene film on Si/SiO_2 is functionalized by surface-initiated ATRP of non-biofouling oligo(ethylene glycol) methacrylate, after grafting of the polymerization initiator bearing α-bromoisobutylate via photoreaction of the perfluorophenyl azide group. The microcontact printing-assisted spatio-selective reaction, after chemical activation of the terminal hydroxyl group of oligo(ethylene glycol) in the polymeric film, is utilized to generate the patterns of fibroblast and hippocampal neurons.

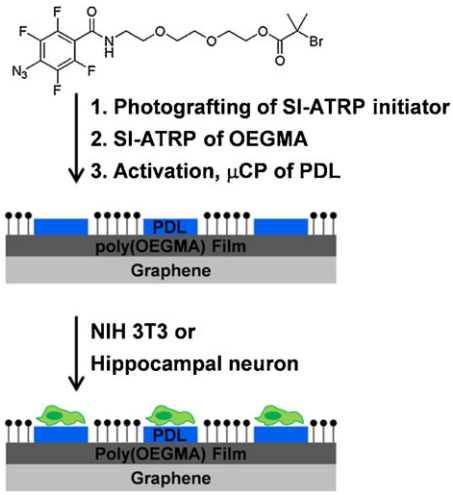

1. Introduction

Graphene, consisting of a single layer of sp^2 carbon atoms, has recently emerged as a new class of 2D materials in the areas of biomedical sciences and biotechnology.[1,2] For example, nanometer-scaled graphene-based materials, including graphene oxide, are incorporated into 3D scaffolds for attachment and proliferation of cells in tissue engineering. A graphene film has been used as a 2D platform for studying cell-material interactions and cellular behaviors, where pristine graphene was mainly used probably due to the limited repertoires for graphene-functionalization methods. The chemical modification of large-area graphene films is still challenging, and some simple reactions, such as hydrogenation,[3–5] fluorination,[6–8] chlorination,[9,10] phenylation,[11] and trimethylsilylation,[12] have so far been demonstrated. However, the biospecific cellular interactions at the material surface require more sophisticated graphene functionalizations that lead to cell-material and cell-cell interactions. Cellular micropatterns on functionalized graphene with one or more cell types would also give useful fundamental information for and provide application platforms in tissue engineering and cell-based sensors, with the unique electrical and chemical properties of graphene. On the other hand, the elasticity and bendability of a graphene sheet (Young's modulus: 0.1–1 TPa) would offer

D. Hong, K. Bae, K. Kang, J. Kim, Prof. S. Kim, Prof. I. S. Choi
Molecular-Level Interface Research Center, Department of Chemistry, KAIST, Daejeon 305-701, Korea
E-mail: ischoi@kaist.ac.kr
S. Yoo, Prof. Y. Nam
Department of Bio and Brain Engineering, KAIST, Daejeon 305-701, Korea
B. Jang, Prof. S. Jeon
Department of Materials Science and Engineering, Graphene Research Center, KAIST, Daejeon 305-701, Korea
Prof. Y.-G. Kim
Department of Chemistry, Sungkyunkwan University, Suwon 440-746, Korea

a flexible modular platform for tissue engineering, after proper modification of graphene surfaces for cell adhesion: for example, the sheet-rolling method for constructing 3D cellular architectures could be applied to the single-layered graphene that is selectively functionalized to have multiple cell patterns.[13] In the aim of controlling the cellular behaviors on a functionalized graphene film, we, in this paper, suggest a simple but versatile method for introducing biologically active moieties onto the graphene surface and, as a demonstration, generate micropatterns of fibroblast and hippocampal neurons on a graphene film.

2. Results and Discussion

Scheme 1 depicts the procedures for generating the cellular micropatterns, consisting of surface-initiated atom-transfer radical polymerization (SI-ATRP), after aryl azide-based photografting of an SI-ATRP initiator, and microcontact printing (μCP). In the SI-ATRP, a polymerization initiator should be introduced onto the surface to be modified before polymerization. Although the formation of self-assembled monolayers (SAMs) terminated with alkyl halide-based initiator (e.g., α-bromoisobutyrate) has efficiently been used for inorganic surfaces, such as gold, silicon dioxide, and titanium dioxide, the formation of SAMs is based on the specific interaction between the functional group of the self-assembling molecule and the surface (e.g., thiol-gold,[14] siloxane-silicon dioxide,[15] phosphate-titanium dioxide,[16] and catechol-titanium dioxide[17]) and cannot be applied to graphene surfaces. Therefore, we used a method of aryl azide-based photografting[18,19] to introduce the polymerization initiator onto the graphene surface.

The large-area (1 cm × 1 cm), single-layered graphene films were prepared according to the previous reports.[20–22] The chemical vapor deposition (CVD)-grown graphene on a Cu foil was transferred to a silicon dioxide (Si/SiO_2) surface, which was used as a reaction platform in this study. We used Raman spectroscopy to characterize the aryl azide-based photografting of the SI-ATRP initiator (**1**) (Figure 1a), because it provides useful information for investigating defects/disorder (D-band), in-plane vibration of sp^2 carbon atoms (G-band), and the stacking orders (2D-band) of graphene.[23] The Raman spectrum of the transferred, intact graphene showed the very weak D band, and the peak intensity ratio of the 2D and G bands was about 4, indicating the high quality of the single-layered graphene film (Figure 1b, black).[24]

The attachment of the SI-ATRP initiator was based on the perfluorophenyl azide (PFPA) chemistry: the photochemical or thermal activation of PFPA generates the highly reactive singlet perfluorophenylnitrene, which undergoes the C=C addition[25] and has been utilized for the solution-based functionalizations of carbon materials, such as fullerene,[26]

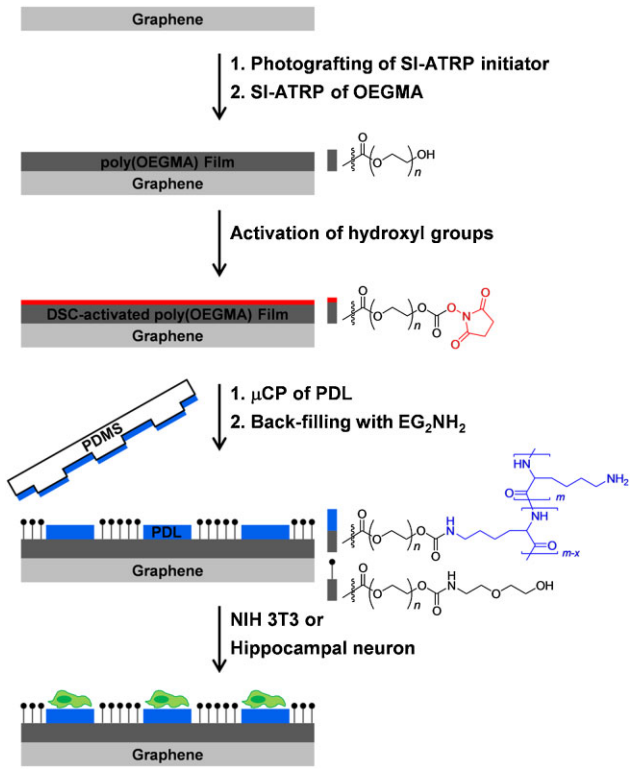

Scheme 1. Procedures for SI-ATRP and generation of cellular patterns.

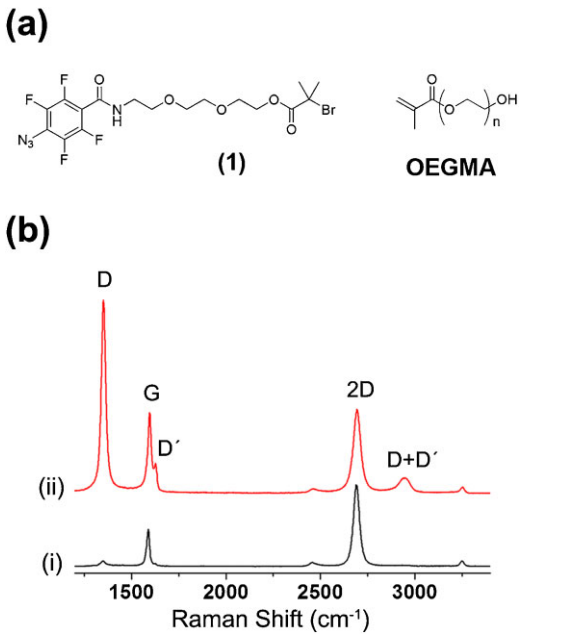

Figure 1. (a) Molecular structures of SI-ATRP initiator, **1**, and OEGMA. (b) Raman spectra of (i) pristine and (ii) ATRP initiator-grafted graphene films.

Macromol. Biosci. **2013,** DOI: 10.1002/mabi.201300346

carbon nanotubes,[27] and graphene.[28] Its chemical reactivity was also used for the covalent immobilization of a graphene sheet onto the silicon wafer presenting PFPA.[29,30] In addition, our previous report with azidotrimethylsilane showed that nitrene formed a covalent bond with epitaxial graphene after thermal activation.[12] Compound **1** was spin-coated on the as-prepared graphene film, followed by 100 s UV irradiation (254 nm). After photografting, the highly intense D band was observed in the Raman spectrum (Figure 1b, red), indicating the destruction of the sp^2 carbon network and the band was accompanied by the D′ band at 1627 cm^{-1}, and the D + D′ band was newly observed around 2942 cm^{-1}.[31] The X-ray photoelectron (XPS) spectrum showed the characteristic peaks of compound **1** at 686.4 (F 1s) and 70.6 eV (Br 3d) after grafting of the initiator (Figure 2a). The water contact angle changed from 42 to 79°, which also indicated the surface modification of graphene (Figure 2b). Taken together, the characterizations confirmed that the SI-ATRP initiator was successively grafted onto the pristine graphene film via photochemical reaction.

After introduction of the initiator, we performed the SI-ATRP of oligo(ethylene glycol) methacrylate (OEGMA) from the graphene film. SI-ATRP has been the most widely used method for grafting polymers from a solid surface since the first demonstration in 1998.[32,33] Various (meth) acrylate- and styrene-based monomers have been employed for SI-ATRP,[34,35] and the polymer-coated surfaces were programmed to possess a multitude of different properties and functions, such as bioinertness,[36,37] bioconjugation,[38–40] anti-microbial properties,[41,42] and even catalysis for mineralization.[43–45] SI-ATRP has especially been successful in generating non-biofouling interfaces against proteins and cells, which contributes to the development of biodevices including microarrays and microfluidic systems by minimizing the non-specific adsorption of proteins and/or the adherence of cells. Oligo(ethylene glycol)-[36–40] or zwitterion-bearing monomers [46–48] have mainly been employed for this purpose. In this work, poly(OEGMA) was chosen because it possesses the non-biofouling property, and, of more importance, can be functionalized chemically for bioconjugation of molecules of interest.[19,39] This dual property of poly(OEGMA) makes it possible to determine the protein (or cell)-attracting and -repelling areas by spatio-selective reactions. The SI-ATRP of OEGMA was performed in a water-methanol solution of bipyridine and Cu(I) bromide for 1 h at room temperature under an argon atmosphere. The water contact angle of poly(OEGMA)-coated graphene was measured to be 55°, indicative of a relatively hydrophilic nature of the polymer film. The terminal hydroxyl group of the OEG side chain was then activated to *N*-hydroxysuccinimide (NHS) by the reaction with *N,N*′-disuccinimidyl carbonate (DSC),[19,39] which subsequently formed the amide linkage with amino groups.

Since poly-D-lysine (PDL) was reported to be effective for the adhesion of cells,[49–51] μCP of PDL-fluorescein isothiocyanate (FITC) was performed onto the activated poly(OEGMA) film with a poly(dimethylsiloxane) (PDMS) stamp that had a grid pattern with 50 μm in width and 150 μm in spacing, and the unreacted square area (150 × 150 μm^2) was passivated with 2-(2-aminoethoxy) ethanol (EG_2NH_2). The passivation restored the cell-resistant property of the film. Figure 3a shows the PDL-FITC pattern, which was visualized by confocal laser scanning microscopy (CLSM). After seeding NIH 3T3 fibroblast cells

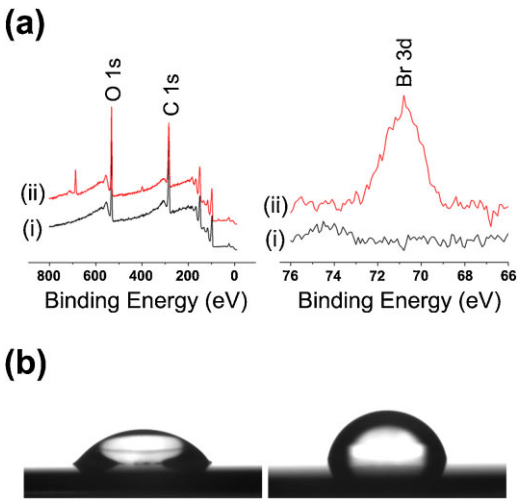

Figure 2. (a) XPS spectra of (i) pristine and (ii) ATRP initiator-grafted graphene films. (b) Water contact angles of (left) pristine and (right) ATRP initiator-grafted graphene films.

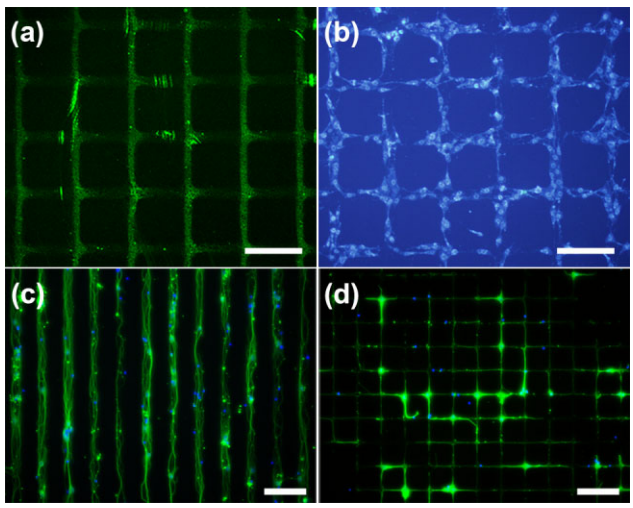

Figure 3. (a) CLSM image of PDL-FITC-patterned graphene film and (b) fluorescence micrograph of NIH 3T3-patterned graphene film. Scale bar: 200 μm. (c and d) Fluorescence micrographs of micropatterns of hippocampal neurons. Scale bar: 100 μm.

Macromol. Biosci. **2013,** DOI: 10.1002/mabi.201300346

at a density of 5×10^5 cells $\cdot$ mL^{-1} and incubating them for 24 h, cells were stained with blue-fluorescent Hoechst 33342: cells adhered and proliferated exclusively on the PDL-functionalized areas (Figure 3b). The structural integrity of the cellular micropatterns also indicated that the single-layered graphene film on Si/SiO_2 was mechanically robust and stable enough to withstand all the chemical and mechanical processes employed in this study.

In addition to the generation of the grid pattern of NIH 3T3 fibroblast cells, the graphene film was also tailored to form a neuronal network. The generation of neuronal network on conductive materials is, in particular, important in the development of the neuron-based sensors and devices that measure the electrophysiological behaviors of neurons.[52] μCP of PDL was performed to generate the line (30 μm in width and 30 μm in spacing) or nodal-grid (node: 16-μm circle; line: 5 μm in width and 50 μm in spacing) patterns: a circular node was made to position the cell body, and the thin lines were designed to guide neurite outgrowth. After μCP, hippocampal neurons from embryonic day 18 (E-18) Sprague-Dawley rat were seeded at a density of 50 cells $\cdot$ mm^{-2} on a PDL-patterned graphene film and cultured in serum-free conditions at 37 °C for 7 d.[53,54] Neurons were immunostained with anti-β tubulin (green), and the location of cell body (soma) was identified with bisbenzimide (blue). Figure 3c and 3d show the fluorescence micrographs of the line and grid patterns of the cultured hippocampal neurons. Figure 3c shows well-confined neuronal growth on the 30 μm-line patterns, where there was no crossing (or bridging) over the repulsive background region. On the more complex nodal grid pattern, cell bodies were mainly located at the circular nodes, and neurites were formed on the 5 μm-lines (Figure 3d). These results confirmed the effective repellency of the poly(OEGMA) film against neurons as well as the successful PDL pattern-generation.

3. Conclusion

In summary, a large-area, pristine graphene film was functionalized by SI-ATRP of OEGMA, and micropatterns of fibroblast and hippocampal neurons were successfully generated by utilizing the non-biofouling but post-functionalizable properties of poly(OEGMA). The PFPA group proved effective in the immobilization of the polymerization initiator on the pristine graphene film, which enabled the subsequent SI-ATRP of OEGMA. Considering the versatility of SI-ATRP, we think that the method demonstrated herein would be utilized in the formation of unprecedented 2D graphene-polymer and even polymer-graphene-polymer architectures as a 2D/3D scaffold for multicell culture, where their biological properties could be tailored by the polymers grafted from each side of graphene.[55] We also believe that the aryl azide-based photochemistry could be applied to a direct, spatio-selective modification of pristine graphene with the aid of conventional photolithographic techniques, while maintaining the intrinsic conducting property of graphene. This direct pattern-generation will particularly contribute to the realization of an in vitro neuronal network, which is our next research thrust.

4. Experimental Section

4.1. Pattern Generation of Poly(OEGMA) on Graphene Films

The CVD-grown, single-layered graphene sheet was transferred onto a silicon wafer or glass and washed with methanol. The graphene film was spin-coated with the initiator **1** (1% w/v in methanol) for 30 s at 1500 rotations per minute (rpm), and the resulting substrate was then irradiated by UV (254 nm) for 100 s. After the substrate was thoroughly washed with methanol several times, SI-ATRP was carried out in the water/methanol (1.34 mL/5.39 mL) solution of OEGMA (3.26 mL, 0.010 mol, Aldrich), Cu(I)Br (143 mg, 1×10^{-3} mol, 99.999%, Aldrich), and 2,2′-bipyridyl (312 mg, 2×10^{-3} mol, >99%, Aldrich) for 1 h at room temperature under an argon atmosphere. After thorough washing with water and methanol, the poly(OEGMA)-coated graphene substrate was immersed in a dry *N*,*N*-dimethylformamide (DMF) solution of DSC (0.1 M) and 4-(dimethylamino)pyridine (DMAP, 0.010 M) for 6 h at room temperature. The sample was thoroughly rinsed with DMF and dried with a stream of argon. The PDMS stamp was oxidized with an oxygen-plasma cleaner (Harrick PDC-002 at medium strength) for 1 min, inked with an aqueous solution of PDL (1 mg $\cdot$ mL^{-1}) by spin-coating, and brought into contact with the activated poly(OEGMA) film for 1 min. After μCP, the remaining succinimidyl moieties were passivated with an aqueous solution of EG_2NH_2 (0.1 mg $\cdot$ mL^{-1}) for 1 h.

4.2. Cell Culture

NIH 3T3 fibroblast cells were maintained in continuous growth in Dulbecco's modified Eagle medium (DMEM), supplemented with 10% fetal bovine serum and 1% antibiotics solution, at 37 °C in a humidified atmosphere containing 5% CO_2 on tissue culture T25 polystyrene flasks. Cells were removed from the flask surface by washing twice with 2 mL of the phosphate-buffered saline solution, followed by incubation of 0.5 mL of 0.25% trypsin/EDTA (ethylendiamine tetraacetic acid) for detachment. The detached cells were resuspended in 2 mL of cell culture media, and the number of cells was counted with a hemocytometer. On the PDL-patterned graphene substrate, placed in a Petri dish, cells were seeded (5×10^5 cells dispersed in 6-mL cell culture media) and incubated at 37 °C in a humidified atmosphere of 5% CO_2. For the cell pattern generation of neurons, the graphene sheet was transferred onto a glass substrate. Primary hippocampal neurons were cultured under serum-free condition. Hippocampi from E-18 Sprague-Dawley rat were triturated in Hank's balanced

Macromolecular Journals

Macromol. Biosci. **2013,** DOI: 10.1002/mabi.201300346

salt solution (HBSS) with a fire-polished Pasteur pipette. The cell suspension was centrifuged for 2 min at 1000 rpm, and a cell pellet was extracted. The cell pellet was suspended in Neurobasal media supplemented with B-27, L-glutamine (2×10^{-3} M), L-glutamic acid (12.5×10^{-6} M), and penicillin-streptomycin using a Pasteur pipette. Dissociated cells were seeded at the density of 50 cells $\cdot$ mm^{-2} on the PDL-patterned graphene substrate. Cells were cultivated in a humidified incubator (37 °C, 5% CO_2).

4.3. Characterizations

Raman spectra were obtained at 514 nm and 0.5 mW incident power with ARAMIS (Horiba Jobin Yvon, France). The XPS study was performed with a Sigma Probe (Thermo VG Scientific, UK) with a monochromatized Al K_α X-ray source (1486.7 eV). Emitted photoelectrons were detected by a multichannel detector at a takeoff angle of 40° relative to the surfaces. Survey spectra were obtained at a resolution of 1 eV from one scan, and high-resolution spectra were acquired at a resolution of 0.1 eV. Contact angle measurements were performed using a Phoenix 300 goniometer (Surface Electro Optics, Korea) on the basis of the sessile drop method. Fluorescence micrographs of cellular micropatterns were obtained with BX51M (Olympus, Japan) equipped with a DP71 CCD camera (Olympus, Japan), and CLSM images with LSM 700 (Zeiss, Germany).

Acknowledgements: This work was supported by the National Research Foundation of Korea (NRF) funded by Ministry of Education, Science, and Technology (2012R1A3A2026403, 20090083525, and 2012R1A2A1A01007327).

Received: July 29, 2013; Revised: September 15, 2013; Published online: DOI: 10.1002/mabi.201300346

Keywords: aryl azide; cells; graphene; micropatterns; surface-initiated polymerization

[1] D. Bitounis, H. Ali-Boucetta, B. H. Hong, D.-H. Min, K. Kostarelos, *Adv. Mater.* **2013**, *25*, 2258.
[2] C. Chung, Y.-K. Kim, D. Shin, S.-R. Ryoo, B. H. Hong, D.-H. Min, *Acc. Chem. Res.* **2013**, *46*, 2211
[3] D. C. Elias, R. R. Nair, T. M. G. Mohiuddin, S. V. Morozov, P. Blake, M. P. Halsall, A. C. Ferrari, D. W. Boukhvalov, M. I. Katsnelson, A. K. Geim, K. S. Novoselov, *Science* **2009**, *323*, 610.
[4] S. Ryu, M. Y. Han, J. Maultzsch, T. F. Heinz, P. Kim, M. L. Steigerwald, L. E. Brus, *Nano Lett.* **2008**, *8*, 4597.
[5] Z. Luo, T. Yu, Z. Ni, S. Lim, H. Hu, J. Shang, L. Liu, Z. Shen, J. Lin, *J. Phys. Chem. C* **2011**, *115*, 1422.
[6] W. H. Lee, J. W. Suk, H. Chou, J. Lee, Y. Hao, Y. Wu, R. Piner, D. Akinwande, K. S. Kim, R. S. Ruoff, *Nano Lett.* **2012**, *12*, 2374.
[7] J. T. Robinson, J. S. Burgess, C. E. Junkermeier, S. C. Badescu, T. L. Reinecke, F. K. Perkins, M. K. Zalalutdniov, J. W. Baldwin, J. C. Culberston, P. E. Sheehan, E. S. Snow, *Nano Lett.* **2010**, *10*, 3001.
[8] R. R. Nair, W. Ren, R. Jalil, I. Riaz, V. G. Kravets, L. Britnell, P. Blake, F. Schedin, A. S. Mayorov, S. Yuan, M. I. Katsnelson, H.-M. Cheng, W. Strupinski, L. G. Bulusheva, A. V. Okotrub, I. V. Grigorieva, A. N. Grigorenko, K. S. Novoselov, A. K. Gein, *Small* **2010**, *6*, 2877.
[9] B. Li, L. Zhou, D. Wu, H. Peng, K. Yan, Y. Zhou, Z. Liu, *ACS Nano* **2011**, *5*, 5957.
[10] J. Wu, L. Xie, Y. Li, H. Wang, Y. Ouyang, J. Guo, H. Dai, *J. Am. Chem. Soc.* **2011**, *133*, 19668.
[11] H. Liu, S. Ryu, Z. Chen, M. L. Steigerwald, C. Nuckolls, L. E. Brus, *J. Am. Chem. Soc.* **2009**, *131*, 17099.
[12] J. Choi, K.-J. Kim, B. Kim, H. Lee, S. Kim, *J. Phys. Chem. C* **2009**, *113*, 9433.
[13] B. Yuan, Y. Jin, Y. Sun, D. Wang, J. Sun, Z. Wang, W. Zhang, X. Jiang, *Adv. Mater.* **2012**, *24*, 890.
[14] Q. Wei, J. Ji, J. Shen, *Macromol. Rapid Commun.* **2008**, *29*, 645.
[15] S. Tugulu, R. Barbey, M. Harms, M. Fricke, D. Volkmer, A. Rossi, H.-A. Klok, *Macromolecules* **2007**, *40*, 168.
[16] B. Barthélémy, S. Devillers, I. Minet, J. Delhalle, Z. Mekhalif, *J. Colloid Interface Sci.* **2011**, *354*, 873.
[17] X. Fan, L. Lin, J. L. Dalsin, P. B. Messersmith, *J. Am. Chem. Soc.* **2005**, *127*, 15843.
[18] J. Kim, D. Hong, S. Jeong, B. Kong, S. M. Kang, Y.-G. Kim, I. S. Choi, *Chem. Asian J.* **2011**, *6*, 363.
[19] S. P. Jeong, D. Hong, S. M. Kang, I. S. Choi, J. K. Lee, *Asian J. Org. Chem.* **2013**, *2*, 568.
[20] S. Bae, H. Kim, Y. Lee, X. Xu, J.-S. Park, Y. Zheng, J. Balakrishnan, T. Lei, H. R. Kim, Y. I. Song, Y.-J. Kim, K. S. Kim, B. Özyilmaz, J.-H. Ahn, B. H. Hong, S. Iijima, *Nat. Nanotechnol.* **2010**, *5*, 574.
[21] Y. Kim, J. Lee, M. S. Yeom, J. W. Shin, H. Kim, Y. Cui, J. W. Kysar, J. Hone, Y. Jung, S. Jeon, S. M. Han, *Nat. Commun.* **2013**, *4*, 2114.
[22] J. Lee, K. Kim, W. I. Park, B.-H. Kim, J. H. Park, T.-H. Kim, S. Bong, C.-H. Kim, G. Chae, M. Jun, Y. Hwang, Y. S. Jung, S. Jeon, *Nano Lett.* **2012**, *12*, 6078.
[23] Y. Y. Wang, Z. H. Ni, T. Yu, Z. X. Shen, H. M. Wang, Y. H. Wu, W. Chen, A. T. S. Wee, *J. Phys. Chem. C* **2008**, *112*, 10637.
[24] A. C. Ferrari, J. C. Meyer, V. Scardaci, C. Casiraghi, M. Lazzeri, F. Mauri, S. Piscanec, D. Jiang, K. S. Novoselov, S. Roth, A. K. Geim, *Phys. Rev. Lett.* **2006**, *97*, 187401.
[25] L.-H. Liu, M. Yan, *Acc. Chem. Res.* **2010**, *43*, 1434.
[26] M. Yan, S. X. Cai, J. F. W. Keana, *J. Org. Chem.* **1994**, *59*, 5951.
[27] S. J. Pastine, D. Okawa, B. Kessler, M. Rolandi, M. Llorente, A. Zettl, J. M. J. Fréchet, *J. Am. Chem. Soc.* **2008**, *130*, 4238.
[28] L.-H. Liu, M. M. Lerner, M. Yan, *Nano Lett.* **2010**, *10*, 3754.
[29] L.-H. Liu, G. Zorn, D. G. Castner, R. Solanki, M. M. Lerner, M. Yan, *J. Mater. Chem.* **2010**, *20*, 5041.
[30] L.-H. Liu, M. Yan, *Nano Lett.* **2009**, *9*, 3375.
[31] S. Niyogi, E. Bekyarova, M. E. Itkis, H. Zhang, K. Shepperd, J. Hicks, M. Sprinkle, C. Berger, C. N. Lau, W. A. deHeer, E. H. Conrad, R. C. Haddon, *Nano Lett.* **2010**, *10*, 4061.
[32] M. Ejaz, S. Yamamoto, K. Ohno, Y. Tsujii, T. Fukuda, *Macromolecules* **1998**, *31*, 5934.
[33] X. Huang, L. J. Doneski, M. J. Wirth, *Anal. Chem.* **1998**, *70*, 4023.
[34] R. Barbey, L. Lavanant, D. Paripovic, N. Schüwer, C. Sugnaux, S. Tugulu, H.-A. Klok, *Chem. Rev.* **2009**, *109*, 5437.
[35] S. Edmondson, V. L. Osborne, W. T. S. Huck, *Chem. Soc. Rev.* **2004**, *33*, 14.
[36] H. Ma, J. Hyun, P. Stiller, A. Chilkoti, *Adv. Mater.* **2004**, *16*, 338.
[37] H. Ma, D. Li, X. Sheng, B. Zhao, A. Chilkoti, *Langmuir* **2006**, *22*, 3751.
[38] B. S. Lee, J. K. Lee, W.-J. Kim, Y. H. Jung, S. J. Sim, J. Lee, I. S. Choi, *Biomacromolecules* **2007**, *8*, 744.
[39] B. S. Lee, Y. S. Chi, K.-B. Lee, Y.-G. Kim, I. S. Choi, *Biomacromolecules* **2007**, *8*, 3922.

[40] S. Tugulu, A. Arnold, I. Sielaff, K. Johnsson, H.-A. Klok, *Biomacromolecules* **2005**, *6*, 1602.
[41] M. Ramstedt, N. Cheng, O. Azzaroni, D. Mossialos, H. J. Mathieu, W. T. S. Huck, *Langmuir* **2007**, *23*, 3314.
[42] S. B. Lee, R. R. Koepsel, S. W. Morley, K. Matyjaszewski, Y. Sun, A. J. Russell, *Biomacromolecules* **2004**, *5*, 877.
[43] S. H. Yang, J. H. Park, W. K. Cho, H.-S. Lee, I. S. Choi, *Small* **2009**, *5*, 1947.
[44] W. K. Cho, S. M. Kang, D. J. Kim, S. H. Yang, I. S. Choi, *Langmuir* **2006**, *22*, 11208.
[45] D. J. Kim, K.-B. Lee, T. G. Lee, H. K. Shon, W.-J. Kim, H-j. Paik, I. S. Choi, *Small* **2005**, *1*, 992.
[46] W. K. Cho, B. Kong, I. S. Choi, *Langmuir* **2007**, *23*, 5678.
[47] W. K. Cho, B. Kong, H. J. Park, J. K. Kim, W. Chegal, J. S. Choi, I. S. Choi, *Biomaterials* **2010**, *31*, 9565.
[48] S. Chen, L. Li, C. Zhao, J. Zheng, *Polymer* **2010**, *51*, 5283.
[49] B. S. Jacobson, D. Branton, *Science* **1977**, *195*, 302.
[50] E. M. Harnett, J. Alderman, T. Wood, *Colloid Surf. B* **2007**, *55*, 90.
[51] K. Kang, G. Kang, B. S. Lee, I. S. Choi, Y. Nam, *Chem. Asian J.* **2010**, *5*, 1804.
[52] M. Lorenzoni, F. Brandi, S. Dante, A. Giugni, B. Torre, *Sci. Rep.* **2013**, *3*, 1954.
[53] K. Kang, S. Lee, R. Kim, I. S. Choi, Y. Nam, *Angew. Chem. Int. Ed.* **2012**, *51*, 13101.
[54] K. Kang, S.-E. Choi, H.-S. Jang, W. K. Cho, Y. Nam, I. S. Choi, J. S. Lee, *Angew. Chem. Int. Ed.* **2012**, *51*, 2855.
[55] L. Zhang, J. Yu, M. Yang, Q. Xie, H. Peng, Z. Liu, *Nat. Commun.* **2013**, *4*, 1443.

Macromol. Biosci. **2013,** DOI: 10.1002/mabi.201300346